Title

Mid-IR laser ablation of articular and fibro-cartilage:A wavelength dependence study of thermal injury and crater morphology



Journal

Lasers in Surgery and Medicine, 38(3)

ISSN

0196-8092

Authors

Youn, Jong-In

Sweet, Paula

Peavy, George M

et al.

Publication Date

2006-03-01

DOI

10.1002/lsm.20288

# Mid-IR Laser Ablation of Articular and Fibro-Cartilage: A Wavelength Dependence Study of Thermal Injury and Crater Morphology

**Jong-In Youn, PhD,[1] Paula Sweet, MT,[1] George M. Peavy, DVM,[1] and Vasan Venugopalan, ScD[1,2]***
[1]*Beckman Laser Institute and Medical Clinic, University of California, Irvine, Irvine, California 92612*
[2]*Department of Chemical Engineering and Materials Science, University of California, Irvine, Irvine, California 92612*

**Background and Objectives:** The aim of this study was to evaluate areas of collateral thermal injury and crater morphology for evidence of wavelength-dependent effects on the ablation of articular cartilage and fibro-cartilage (meniscus) using selected mid-IR wavelengths produced by a free electron laser.

**Study Design/Materials and Methods:** Two types of cartilage, articular cartilage and fibro-cartilage were used in the study. The wavelengths ($\lambda$) evaluated were 2.79, 2.9, 6.1, and 6.45 μm generated by a free electron laser (FEL) using a 4 microseconds macropulse configuration. The zone of thermal injury and crater morphology produced by laser ablation were examined by light microscopy following standard histologic processing.

**Results:** The zone of thermal injury and crater morphology created in cartilage by the FEL at selected mid-IR wavelengths were examined as a function of incident radiant exposure. Ablation using $\lambda = 6.1$ μm provided the largest crater size for both articular and fibro-cartilage at all radiant exposures. For the zones of collateral thermal injury in articular cartilage, $\lambda = 6.1$ μm produced the least thermal injury at the radiant exposure of 7.6 J/cm$^2$. When the radiant exposure is increased to 20.4 J/cm$^2$, both $\lambda = 6.1$ and 6.45 μm produced less thermal injury than the ablation using $\lambda = 2.79$ and 2.9 μm. The greatest amount of collateral thermal injury was produced by $\lambda = 2.79$ μm for both tissue types.

**Conclusions:** The results demonstrate that crater depth and collateral thermal injury produced in articular cartilage and fibro-cartilage are wavelength-dependent with 6.1 μm providing the largest craters at all radiant exposures. The least amount of thermal injury was created in articular cartilage using $\lambda = 6.1$ μm at the radiant exposure of 7.6 J/cm$^2$. Both 6.1 and 6.45 μm wavelengths demonstrated similar amount of thermal injury at 20 J/cm$^2$ that was less than $\lambda = 2.79$ and 2.9 μm at similar fluences. These observations are explained based on the absorption by water and protein in the tissue types studied. It is further observed that the use of crater dimensions may not provide a reliable estimate for the amount of tissue removal provided by an ablation procedure. Lasers Surg. Med. 38:218–228, 2006. © 2006 Wiley-Liss, Inc.

**Key words:** ablation; articular cartilage; crater; fibro-cartilage; free electron laser; laser; meniscus; thermal injury

## INTRODUCTION

Over the past few decades, lasers have found access to a variety of medical fields. Lasers have been evaluated in arthroscopic surgical procedures of the knee for the treatment of injured articular cartilage and torn meniscus tissue as a means of achieving controlled removal of tissue with minimal collateral thermal injury [1–20]. While an early investigation of the Nd:YAG laser ($\lambda = 1064$ nm) effects on articular cartilage and meniscus reported that the damage characteristics and healing response produced by the Nd:YAG laser were advantageous over scalpel and electrocautery, the zones of thermal injury were not specifically addressed and no histologic quantification of results were provided [1]. An investigation of the effect of varying Ho:YAG laser ($\lambda = 2.1$ μm) parameters on ablation of bovine knee joint tissues found that zones of thermal injury varied between tissue types, but were independent of the fluence, pulse width, and fiber size [7]. A study using five different laser systems [XeCl Excimer ($\lambda = 308$ nm), KTP ($\lambda = 532$ nm), Nd:YAG, Ho:YAG and $CO_2$ ($\lambda = 10.6$ μm)] and electrocautery by Vangsness et al. [11] indicated that the KTP laser produced the least thermal injury zone and that electrocautery produced the roughest surface, which was pitted and jagged. Bernard et al. [16] also examined cartilage ablation using several laser systems reporting that the XeCl excimer laser provided minimal thermal injury, but ablation rates and cutting efficiency were lower than other laser systems. While the studies by Vangsness et al. and Bernard et al. provided general ablation characteristics produced by various laser systems, no systematic correlation was made between specific laser

Contract grant sponsor: U.S. Air Force Office of Scientific Research (Medical Free-Electron Laser Program); Contract grant numbers: F49620-00-1-0371, FA9550-04-1-0101; Contract grant sponsor: The National Center for Research Resources of the National Institutes of Health (Laser Microbeam and Medical Program); Contract grant number: RR-01192; Contract grant sponsor: Arnold and Mabel Beckman Foundation.

*Correspondence to: Vasan Venugopalan, ScD, Department of Chemical Engineering and Materials Science, Beckman Laser Institute and Medical Clinic, University of California, Irvine, Irvine, CA 92612. E-mail: vvenugop@uci.edu

Accepted 22 November 2005
Published online 1 February 2006 in Wiley InterScience (www.interscience.wiley.com).
DOI 10.1002/lsm.20288

parameters (i.e., pulse duration ($\tau$), repetition rate ($f$), incident radiant exposure ($\Phi$), and spot diameter) and the resultant ablation characteristics [11,16]. Since the early 1990s, cartilage ablation studies have focused on the Er:YAG laser ($\lambda = 2.94$ μm) because its wavelength is strongly absorbed by water and results in minimal thermal injury [18–20]. Gonzales et al. [18] conducted a comparison of Er:YAG and $CO_2$ laser ablation of cartilage and indicated that the Er:YAG laser efficiently ablates cartilage with significantly less thermal injury. The effects of Ho:YAG and Er:YAG laser pulses ($\tau = 400$ microseconds) on chondrocyte viability using different energy levels also demonstrated that thermal injury was greater with Ho:YAG (~1,800 μm) than with the Er:YAG laser (~70 μm) [19]. The thermal injury and crater size produced by Ho:YAG and Er:YAG laser ablation was also quantified by confocal microscopy, demonstrating that larger zones of thermal injury and smaller ablation depths were achieved using the Ho:YAG laser as compared to the Er:YAG laser [20].

Previous studies suggest that the use of $\lambda = 2.9$ μm due to optical absorption by the water OH-stretch mode results in explosive vaporization and provides an efficient process for cartilage ablation [4,18–20]. Vogel and Venugopalan considered the temperature dependence of the optical properties of water. Their analysis revealed that for radiant exposures in the range of 0.1–10 J/cm$^2$, the optical penetration depth of $\lambda = 2.79$ μm radiation is in fact lower than $\lambda = 2.94$ μm. As a result, it is possible that ablation using Er:YSGG ($\lambda = 2.79$ μm) offers better spatial confinement of the deposited laser energy and resultant thermal injury than $\lambda = 2.94$ μm radiation under certain conditions [21]. In this study, both 2.79 and 2.9 μm wavelengths were chosen to examine this possibility.

A wavelength-dependent study of tissue ablation is essential because the optical absorption properties of the tissue are important factors that affect crater depth and collateral thermal injury. While water is the dominant chromophore in tissue, the direct targeting of protein may provide increased ablation efficiency with less collateral thermal injury through protein modification. Several studies have indicated that wavelengths absorbed by tissue matrix instead of, or in addition to, the tissue water may prove advantageous in increasing ablation rate and reducing collateral thermal injury [22–32]. Using the unique pulse structure of an FEL tuned to several wavelengths between 3.0 and 6.85 μm, Edwards et al. [22] were the first to report that the optimal wavelength, as determined by ablation yield and collateral thermal damage, was 6.45 μm for cornea and neural tissue, and in the range of 6.0–6.45 μm for dermis. Many investigators since then have used the FEL to target tissue matrix at the Amide I (~6.1 μm), Amide II (~6.45 μm), and/or Amide III (~7.87 μm) absorption peaks to examine ablation characteristics as a function of wavelength [23–32]. Although Edwards et al. demonstrated that the $\lambda = 6.45$ μm provided good ablation yield with little collateral thermal injury, several studies using an FEL to examine wavelength dependence have indicated that $\lambda = 6.1$ μm rather than $\lambda = 6.45$ μm radiation provides the best ablation efficiency with the least amount of collateral thermal injury [24,27,30–32]. In the present study, both 6.1 and 6.45 μm wavelengths were chosen to examine the targeting of protein and water simultaneously on the one hand and primarily tissue protein on the other. We have previously investigated the mass removal of articular and fibrocartilage at selected mid-IR wavelengths (2.79, 2.9, 6.1, and 6.45 μm) and found that $\lambda = 6.1$ μm provided the greatest ablation efficiency in both types of cartilage [32]. In this study, detailed information regarding thermal injury and crater morphology following mid-IR FEL ablation at these wavelengths is presented.

## MATERIALS AND METHODS

A mid-infrared FEL tuned to one of the four wavelengths of interest, 2.79, 2.9, 6.1 or 6.45 μm, delivered in 4 microseconds duration macropulses at a repetition rate of either 5 or 10 Hz was used for this study. The radiant exposure delivered to the tissue was set to predetermined values between 7.6 and 20.4 J/cm$^2$ using a custom-made germanium attenuator, and confirmed by an energy meter (EM 500, Molectron Inc., Portland, OR). The optical arrangement was as previously described using a beam diameter of $500 \pm 10$ μm at the target surface as measured directly for each wavelength by use of a custom-designed motorized knife-edge instrument [32]. The patella, distal femur, proximal tibia, and both menisci were isolated from fresh bovine cadaver knees obtained from a local abattoir. Individual specimens were harvested by 4-mm biopsy punch wrapped in 0.9% saline-soaked gauze sponges, placed in sealed plastic bags and refrigerated until used. Each sample was placed in a sealed container of 10% phosphate-buffered formalin and refrigerated for histology following ablation.

For histologic analysis, samples were rinsed and placed in a phosphate-buffered saline solution and then gross photomicrographs were made using an Olympus SZH microscope (Olympus America, Inc., Melville, NY) with an Olympus MicroFire digital imaging system (Olympus America, Inc.). Following photography, the samples were imbedded in paraffin and processed for histology. Serial sections were cut perpendicular to the tissue surface at 6 μm intervals, mounted on 1×3 inch glass slides and stained with Hematoxylin and Eosin-y (H&E).

For analysis of crater morphology, the section of each specimen with the deepest crater was identified and photographed using light microscopy (Olympus BH-2, Olympus America, Inc.) and a MicroFire digital imaging system (Olympus America, Inc.). The width, depth, and area of the crater were measured using IP Lab (Scanalytics, Inc., Fairfax, VA). The IP Lab program was also used to measure the zone of thermal injury at three points; the base of the crater and the mid-point of each side of the crater perpendicular to the surface of the crater as shown in Figure 1. The measured values of crater width, depth, cross-sectional area, and the zones of thermal injury at all incident radiant exposures tested were compared by statistical $t$-test (two-tailed).

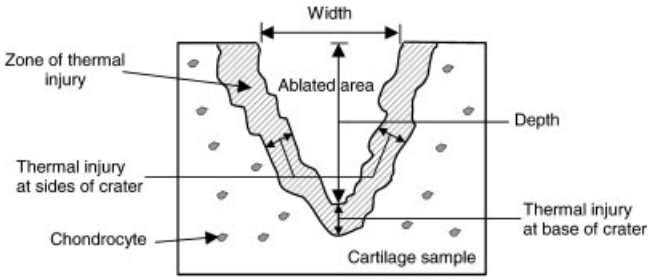


Fig. 1. Schematic of measurements of crater width, depth, and the zones of thermal injury at the base of the crater and the mid-point of each side of the crater perpendicular to the crater surface. The error bars are standard deviations.

## RESULTS

Figure 2 presents light micrographs of typical histological sections following ablation of articular cartilage at $\Phi = 7.6$ J/cm$^2$ at each of four wavelengths. Histological examination of articular cartilage after $\lambda = 6.1$ μm FEL ablation at 7.6 J/cm$^2$ revealed zones of thermal injury of less than 15 μm (Fig. 2C). In contrast, thermal injury zones at the other three wavelengths (2.79, 2.9, and 6.45 μm) were more prominent ranging from 30 μm to 80 μm with the largest zone of thermal injury observed for $\lambda = 2.79$ μm (~80 μm). Figure 3 presents typical sections of articular cartilage for a radiant exposure of 20.4 J/cm$^2$. At this high radiant exposure, $\lambda = 6.1$ μm produced the largest crater size. Both $\lambda = 6.1$ and 6.45 μm produced the least thermal injury at the crater bottom (~30 μm) and side (~10 μm) as compared to the other two wavelengths (Figs. 3 and 4).

Quantitative measurements of thermal injury on the side and bottom of the ablation craters are provided in Table 1 (Fig. 4A) and Table 2 (Fig. 4B), respectively. At 7.6 J/cm$^2$, $\lambda = 2.79$ μm produced the greatest thermal injury along the crater sides ($P<0.01$) was found and $\lambda = 6.1$ μm produced the least thermal injury ($P<0.01$). For $\Phi = 20.4$ J/cm$^2$, we found similarly that the greatest thermal injury was produced at $\lambda = 2.79$ μm ($P<0.01$), but a minimal amount of thermal injury was produced at both $\lambda = 6.1$ μm and $\lambda = 6.45$ μm (Table 1, Fig. 4A) with no statistical difference between them. For the crater and base at $\Phi = 7.6$ J/cm$^2$, the greatest thermal injury was found at $\lambda = 2.79$ μm ($P<0.03$) and the least at $\lambda = 6.1$ μm ($P<0.01$). However, at $\Phi = 20.4$ J/cm$^2$, the thermal injury provided by $\lambda = 6.1$ μm and $\lambda = 6.45$ μm are essentially equivalent (Table 2, Fig. 4B). In Figure 5, we present (A) the width, (B) depth, and (C) cross-sectional area of the ablation craters for each wavelength as a function of radiant exposure. Figure 5A shows that the ablated craters formed by $\lambda = 6.1$ and 6.45 μm are wider as compared to those created at $\lambda =$ 2.79 and 2.9 μm. Analysis of the data in Figure 5B reveals no correlation between crater depth and wavelength with increasing incident radiant exposure. For a fixed radiant exposure, there was no statistically significant difference in the cross sectional area of the ablated craters at $\lambda = 2.79$,

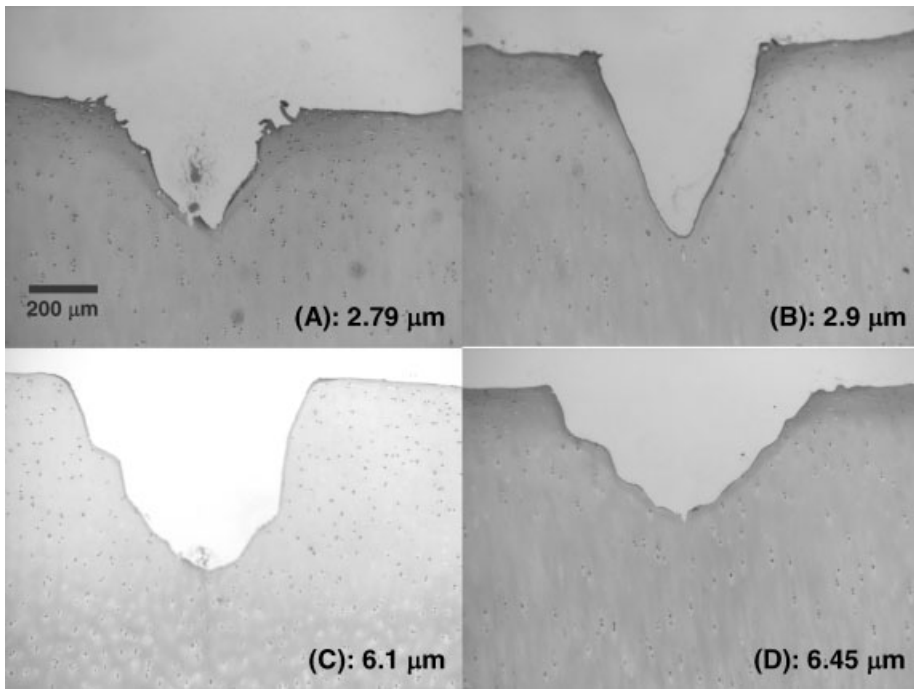


Fig. 2. Histologic sections of articular cartilage ablation craters created using 7.6 J/cm$^2$ for each of four different wavelengths; (**A**) 2.79 μm, (**B**) 2.9 μm, (**C**) 6.1 μm, and (**D**) 6.45 μm.

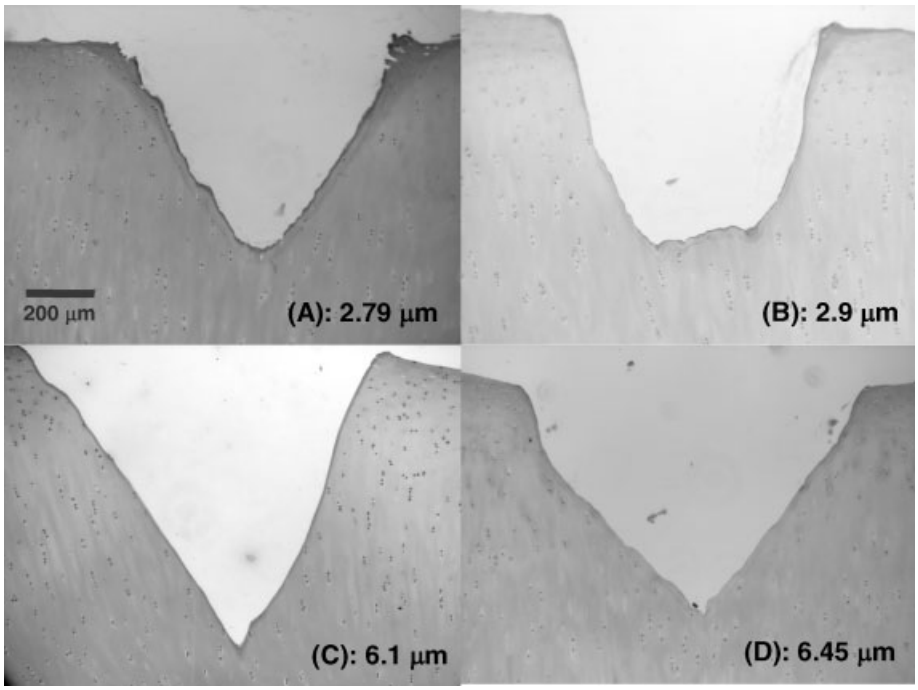


Fig. 3. Histologic sections of articular cartilage ablation craters created using 20.4 J/cm$^2$ for each of four different wavelengths; (**A**) 2.79 μm, (**B**) 2.9 μm, (**C**) 6.1 μm, and (**D**) 6.45 μm.

2.9, and 6.45 μm, however, there was a significantly greater crater area produced by $\lambda = 6.1$ μm ($P<0.01$) (Fig. 5C).

Figure 6 presents typical sections produced by ablation of fibro-cartilage at $\Phi = 7.6$ J/cm$^2$. Ablation at $\lambda = 2.79$ μm produced significant thermal injury (>180 μm) along the fibers in the upper region of the crater (Fig. 6A). The least thermal injury (<10 μm) was observed at $\lambda = 6.1$ μm (Fig. 6C). Figure 7 shows sections of typical craters produced at $\Phi = 20.4$ J/cm$^2$. Ablation at $\lambda = 2.79$ μm occasionally produced an area of char with much thermal injury (> 80 μm) (Fig. 7A). In contrast, the least thermal injury (<10 μm) was observed at $\lambda = 6.1$ μm (Fig. 7C).

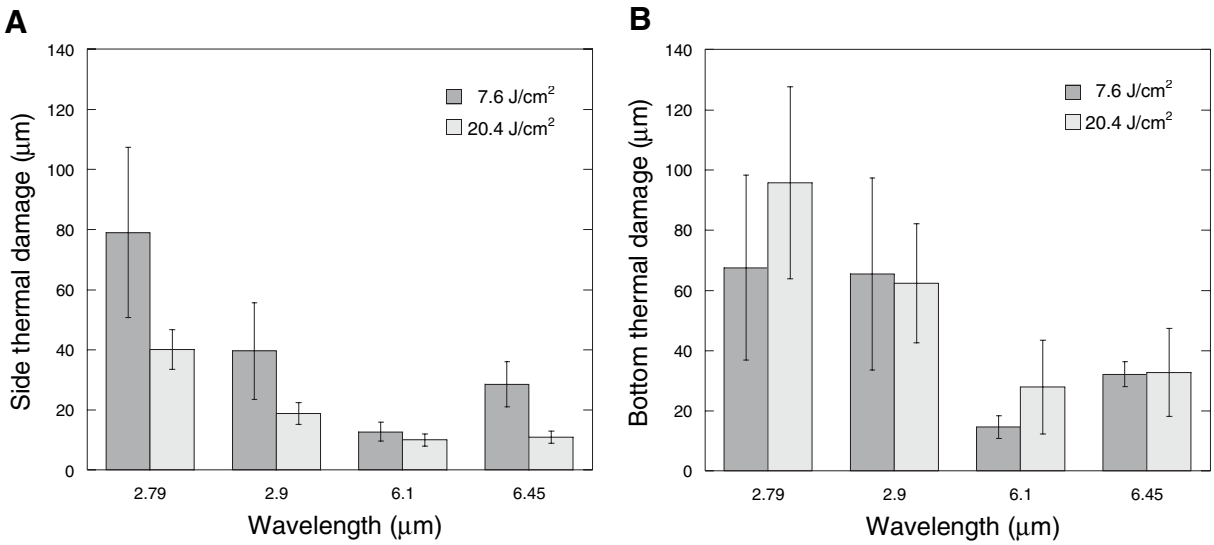


Fig. 4. Zones of thermal injury for articular cartilage (μm) at 7.6 J/cm$^2$ and 20.4 J/cm$^2$; (**A**) width of thermal injury at side, and (**B**) width of thermal injury at base of crater. The error bars are standard deviations of the data.

**TABLE 1. Quantitative Measurements of Thermal Injury at the Sides of Ablation Craters Made in Articular Cartilage Using 2.79, 2.9, 6.1, and 6.45 μm Laser Wavelengths. For Each Parameter, $n = 5$**

| $\Phi$ | $\lambda = 2.79$ μm | $\lambda = 2.9$ μm | $\lambda = 6.1$ μm | $\lambda = 6.45$ μm |
|---|---|---|---|---|
| 7.6 J/cm$^2$ | 80 ± 28 μm | 40 ± 20 μm | 13 ± 3 μm | 29 ± 8 μm |
| 20.4 J/cm$^2$ | 40 ± 7 μm | 19 ± 4 μm | 10 ± 2 μm | 11 ± 2 μm |

**TABLE 2. Quantitative Measurements of Thermal Injury at the Base of Ablation Craters Made in Articular Cartilage Using 2.79, 2.9, 6.1, and 6.45 μm Laser Wavelengths. For Each Parameter, $n = 5$**

| $\Phi$ | $\lambda = 2.79$ μm | $\lambda = 2.9$ μm | $\lambda = 6.1$ μm | $\lambda = 6.45$ μm |
|---|---|---|---|---|
| 7.6 J/cm$^2$ | 70 ± 30 μm | 70 ± 30 μm | 15 ± 4 μm | 32 ± 4 μm |
| 20.4 J/cm$^2$ | 100 ± 30 μm | 60 ± 20 μm | 30 ± 20 μm | 30 ± 20 μm |

Ablation craters produced in fibro-cartilage by all four wavelengths resulted in an irregular variation of thermal injury around the sides of the craters (Fig. 7). Unlike articular cartilage, meniscus is a fibro-cartilaginous tissue composed of an interlacing network of distinct collagen fibers. Thermal energy generated in fibro-cartilage subsequent to laser irradiation is transferred along the collagen fibers producing a highly irregular and spatially varying zone of thermal injury at both side and bottom regions of the craters that is dependent upon the local

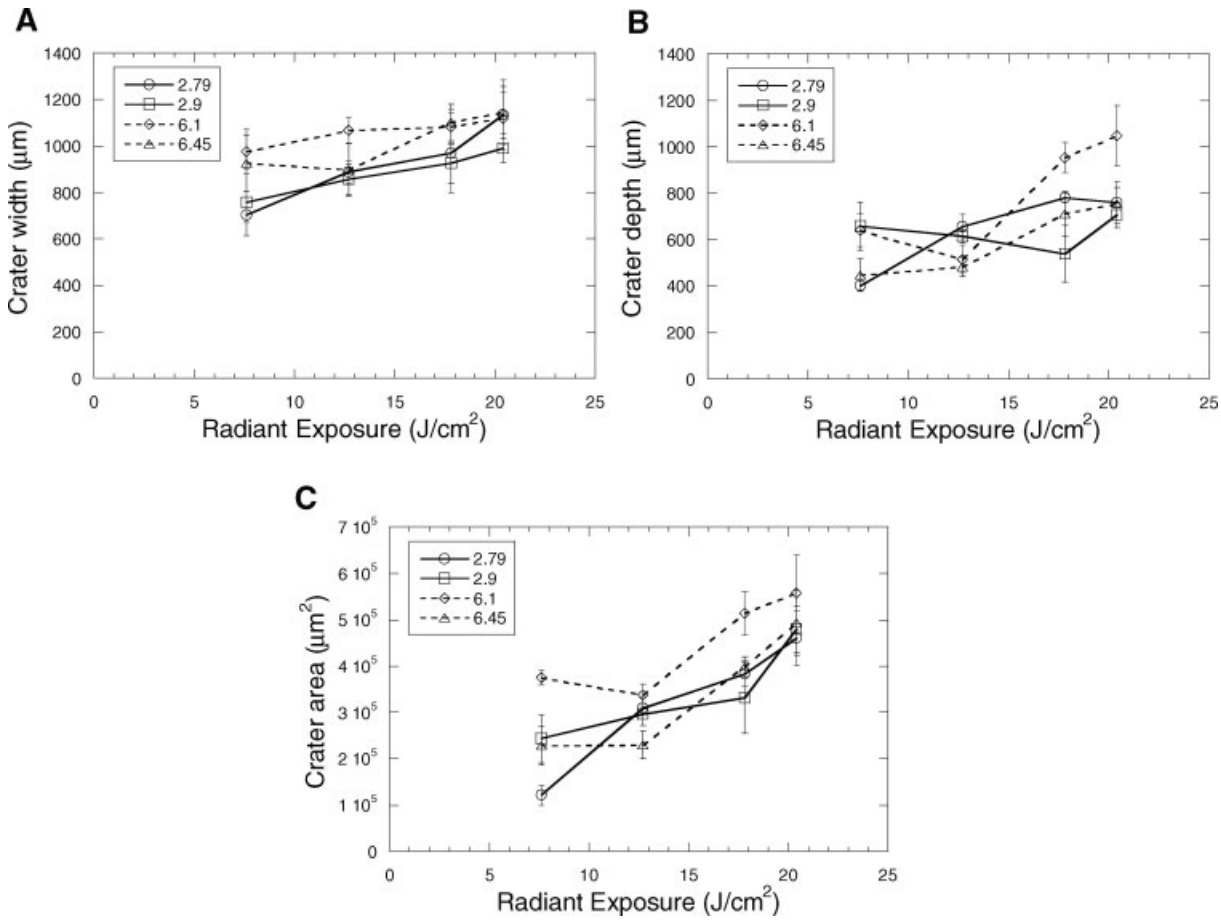


Fig. 5. Crater geometry measurements of articular cartilage versus incident radiant exposure; (**A**) width at surface, (**B**) depth, and (**C**) area of the craters. The error bars are standard deviations of the data.

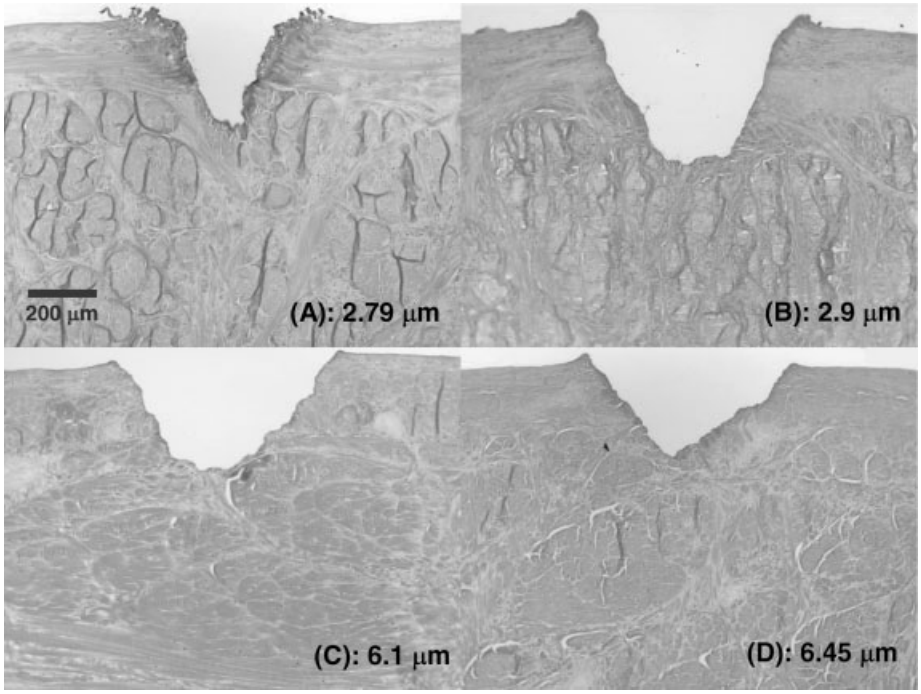


Fig. 6. Histologic sections of fibro-cartilage ablation craters created using 7.6 J/cm$^2$ for each of four different wavelengths; (**A**) 2.79 μm, (**B**) 2.9 μm, (**C**) 6.1 μm, and (**D**) 6.45 μm.

orientation of the collagen fibers (Figs. 6 and 7). This high variability precluded us from providing meaningful quantitative measurements of thermal injury for fibro-cartilage.

Figure 8 provides the quantitative measurements of the crater morphology for fibro-cartilage ablation. The greatest crater width and area were observed at $\lambda = 6.1$ μm with the exception of the outlying data point at $\Phi = 17.8$ J/cm$^2$ (Fig. 8A,C), however, no correlation was found between wavelength and crater depth produced with increasing incident radiant exposure (Fig. 8B).

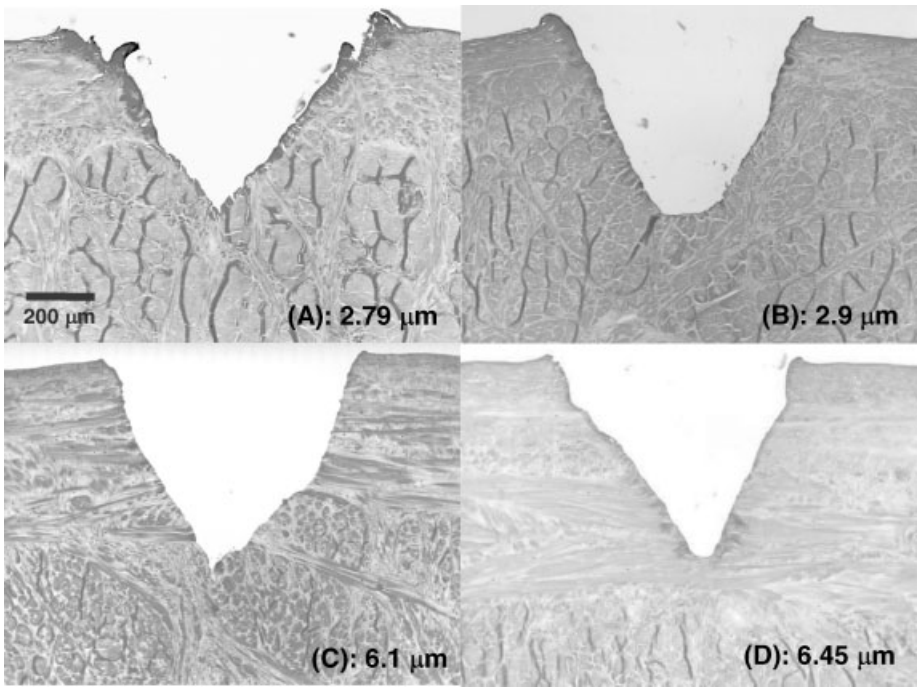


Fig. 7. Histologic sections of fibro-cartilage ablation craters created using 20.4 J/cm$^2$ for each of four different wavelengths; (**A**) 2.79 μm, (**B**) 2.9 μm, (**C**) 6.1 μm, and (**D**) 6.45 μm.

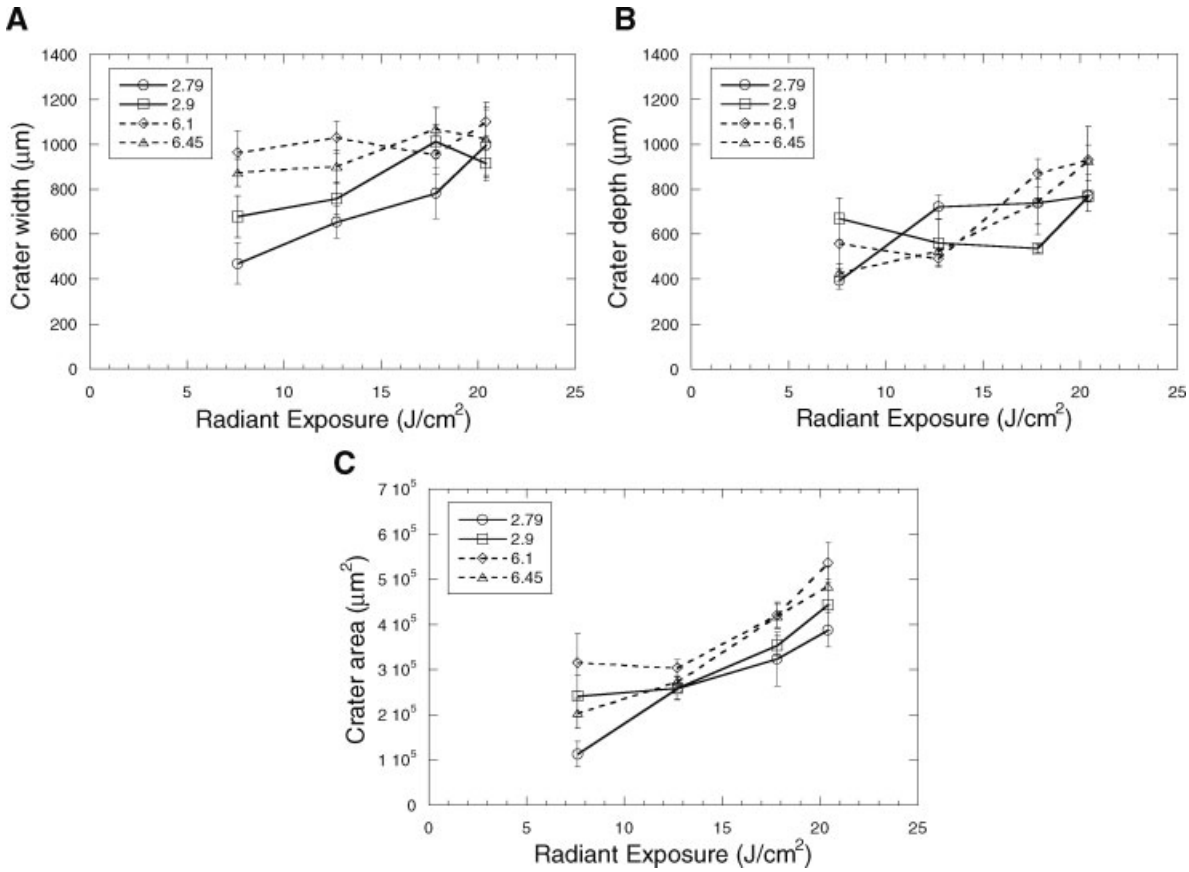


Fig. 8. Crater geometry measurements of fibro-cartilage versus incident radiant exposure; (**A**) width, (**B**) depth, and (**C**) cross-sectional area of the craters for all four wavelengths tested. The error bars are standard deviations of the data.

## DISCUSSION

Cartilage is an avascular tissue consisting of chondrocytes and extracellular matrix composed of predominantly water and protein (proteoglycan aggrecans and collagen) [33–36]. The water and protein content differ significantly between cartilage types as articular cartilage contains 70% water and 30% protein while fibro-cartilage contains 55% water and 45% protein [36]. Optical absorption is one of the important factors affecting ablation dynamics and the resultant thermal injury. Water is the principal constituent in cartilage and is the strongest optical absorber overall in the IR spectral region.

Although water is the dominant chromophore in soft tissue, proteins can act as important chromophores at specific mid-IR wavelengths. Many experimental investigations using a variety of tissues have been performed using a FEL because of its broad wavelength tunability [22–32]. The relationship between optical absorption and collateral thermal injury has been investigated as a function of wavelength using FEL irradiation, and has demonstrated that the collateral thermal injury decreases with increasing optical absorption [25,26,28,29]. Fowler et al. [27] found that the least amount of collateral thermal injury during corneal ablation was achieved when using $\lambda = 6.1$ μm. Heya et al. [30] demonstrated that gelatin with 80 wt% water was most efficiently ablated by a FEL when using $\lambda = 6.1$ μm. Mackanos et al. [31] provided a histological analysis of corneal and dermal tissue to determine thermal injury at $\lambda = 6.1$ μm and $\lambda = 6.45$ μm using 1 ps and 200 ps FEL pulses and found that $\lambda = 6.1$ μm showed significantly less thermal injury on both tissue types as compared to $\lambda = 6.45$ μm. No significant difference in thermal injury was found between the two different pulse durations [31].

The thermal injury and crater morphology of articular and fibro-cartilage reported in this study demonstrate that the largest crater area with the least amount of collateral thermal injury is produced in both cartilage types when using $\lambda = 6.1$ μm. The 6.1-μm wavelength is highly absorbed by both protein ($\mu_a = 2{,}700$ /cm) and water ($\mu_a = 8{,}480$ /cm). Delivery of $\lambda = 6.1$ μm radiation in 4 microsecond macropulses to articular cartilage produced regions of thermal injury of less than 40 μm on both the crater side and base.

The water molecule vibrates in a number of modes and characteristic absorption bands exist at $\lambda = 2.9$ and 6.1 μm

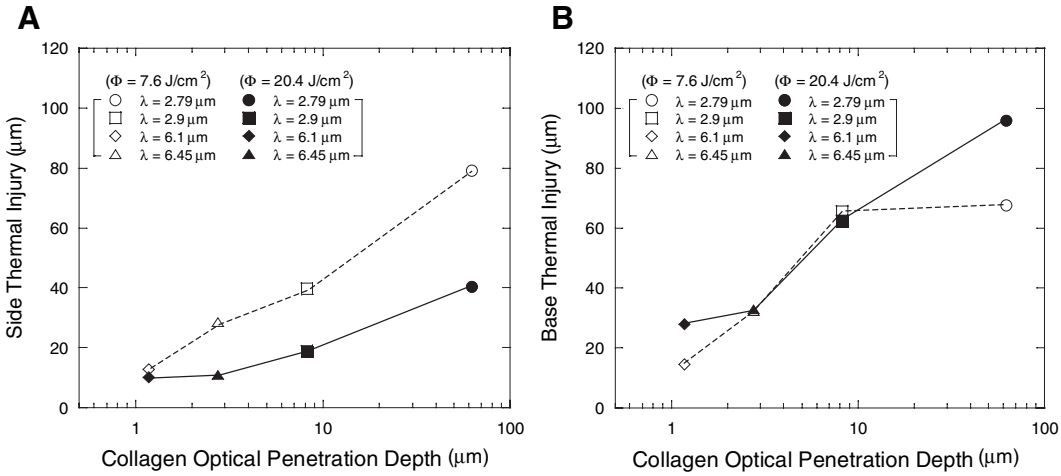


Fig. 9. Collateral thermal injury of articular cartilage versus optical penetration depth of collagen at the corresponding wavelengths, 2.79, 2.9, 6.1, and 6.45 μm; (**A**) width of thermal injury at side, and (**B**) width of thermal injury at base of crater.

[37]. The main absorption bands of protein arise from the peptide bond vibrations at $\lambda = 6.024–6.097$ μm and $\lambda = 6.451–6.514$ μm referred to as Amide I and II, respectively [38]. Due to its larger water content, the absorption coefficients of articular cartilage are higher than those of fibro-cartilage at $\lambda = 2.79$ and 2.9 μm. By contrast, higher absorption coefficients are observed for fibro-cartilage than for articular cartilage at $\lambda = 6.1$ and 6.45 μm due to its higher protein content.

Figures 9 and 10 present the thermal injury produced at the side and base of the ablation crater in articular cartilage versus the optical penetration depth ($1/\mu_a$) of collagen (Fig. 9) and water (Fig. 10). For both crater side (Fig. 9A) and base (Fig. 9B), there is a clear, monotonic increase in thermal injury with increasing optical penetration depth of collagen suggesting that high absorption by collagen results in less collateral thermal injury. This finding is consistent with soft-tissue studies for which less collateral thermal injury has been demonstrated when using wavelengths that target the principal chromophores such as protein and water [22–30]. No correlation was found between the optical penetration depth of water and thermal injury produced in articular cartilage (Fig. 10).

The histologic analysis of both articular and fibro-cartilage revealed that laser ablation at $\lambda = 2.79$ μm produces the greatest amount of thermal injury. It has been shown that the absorption peak of water at $\lambda = 2.94$ μm shifts toward the shorter wavelengths as the water

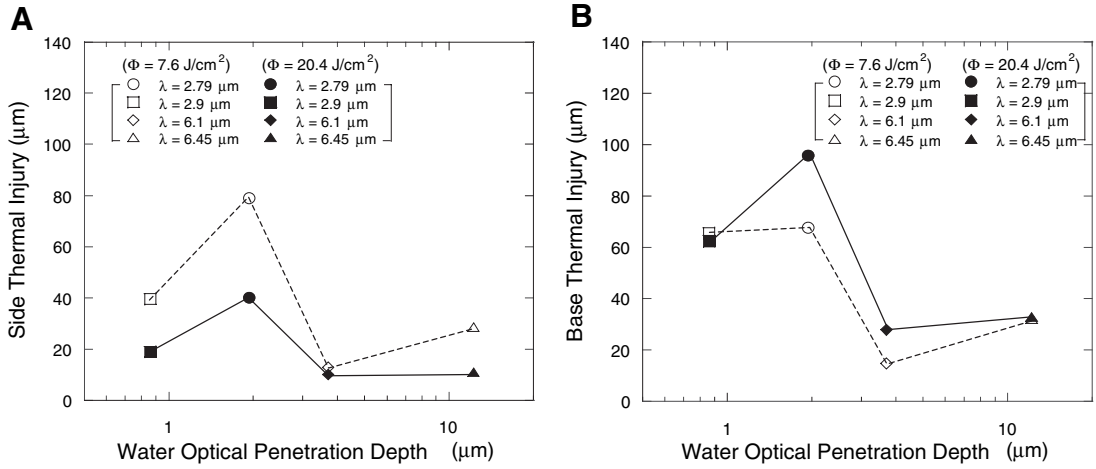


Fig. 10. Collateral thermal injury of articular cartilage versus optical penetration depth of water at the corresponding wavelengths, 2.79, 2.9, 6.1, and 6.45 μm; (**A**) width of thermal injury at side, and (**B**) width of thermal injury at base of crater.

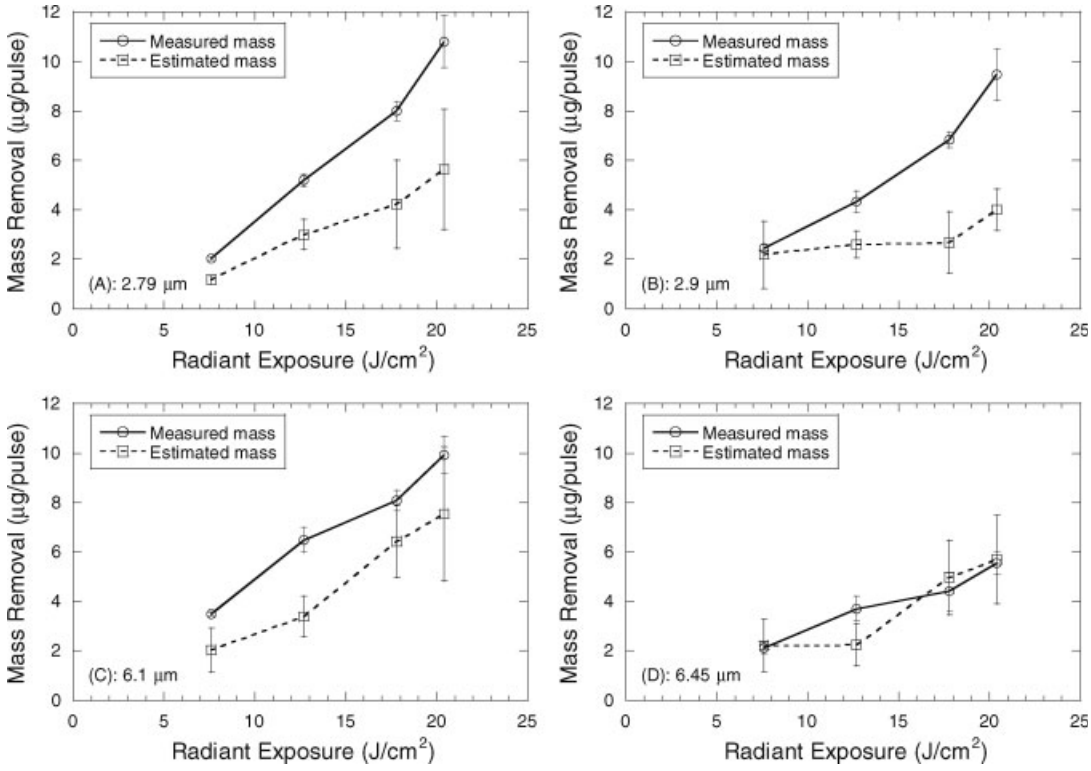


Fig. 11. Mass removal versus incident radiant exposure of articular cartilage for measured mass by a microbalance (solid line) and estimated mass by crater geometry (dotted line) with four different wavelengths; (**A**) 2.79 μm, (**B**) 2.9 μm, (**C**) 6.1 μm, and (**D**) 6.45 μm. The error bars are standard deviations of the data.

temperature is increased due to the weakening of the hydrogen bonds between adjacent water molecules [39,40]. Earlier analysis of Vogel and Venugopalan demonstrated that $\lambda = 2.79$-μm radiation offers better spatial confinement of the laser energy than $\lambda = 2.94$ μm radiation when the incident radiant exposures are between 0.1 J/cm$^2$ and 10 J/cm$^2$ [21]. In our presented histology analysis, the greatest amount of thermal injury shown in both cartilage types at $\lambda = 2.79$ μm, where radiant exposures are larger than 7 J/cm$^2$, may be due to its larger optical penetration depth at these higher radiant exposures.

Our previous study of mass removal of articular and fibro-cartilage produced by FEL ablation at 2.79, 2.9, 6.1, and 6.45 μm found that the $\lambda = 6.1$ μm provided the greatest ablation efficiency [32]. Figure 11 (articular cartilage) and Figure 12 (fibro-cartilage) show a comparison of the measured tissue mass removal conducted using a microbalance during laser ablation from our previous studies with an estimated mass removal based upon the area of the crater geometry. By assuming the craters produced by laser ablation to be inverted cone shapes, the mass removed from the ablation can be estimated by multiplying the calculated crater volume by the tissue density (1.1 g/cm$^3$) obtained from the literature [41,42]. The calculated mass removal consistently underestimates the measured mass removal, however, the mass removal estimated from crater dimensions exhibits the same trends as the measured mass removal in both articular and fibro-cartilage with the exception of the data generated by $\lambda = 6.45$ μm in articular cartilage. Histology is an important tool for the evaluation of collateral thermal injury in the tissue, as well as describing crater shape and depth, but the observed crater shape and depth are highly dependent upon many factors, including the region of sectioning, orientation of the sectioning to the crater geometry, and tissue deformation involved in geometrical fixation and mounting of sections. Because of the inherent alteration of tissue by processing, the measurement of tissue mass removed during laser ablation using a microbalance is a more accurate and reliable measurement of ablation efficiency.

## CONCLUSION

The results were found to be dependent upon wavelength with $\lambda = 6.1$ μm being the most efficient wavelength for ablative removal of cartilage. Furthermore, ablation of articular cartilage using $\lambda = 6.1$ μm created the least amount of collateral thermal injury at the radiant exposure of 7.6 J/cm$^2$ but approached that of $\lambda = 6.45$ μm at 20.4 J/cm$^2$. The greatest amount of thermal injury was observed for both cartilage tissue types at $\lambda = 2.79$ μm. Direct measurement of

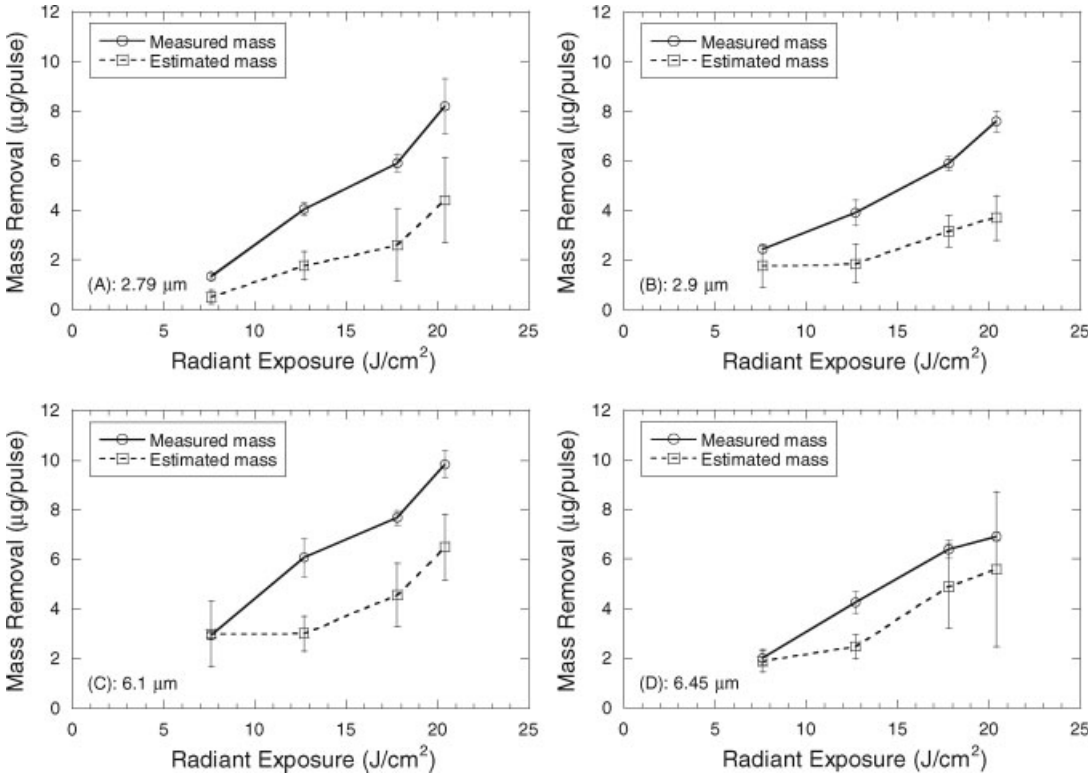


Fig. 12. Mass removal versus incident radiant exposure of fibro-cartilage for measured mass by a microbalance (solid line) and estimated mass by crater geometry (dotted line) with four different wavelengths; (**A**) 2.79 µm, (**B**) 2.9 µm, (**C**) 6.1 µm, and (**D**) 6.45 µm. The error bars are standard deviations of the data.

tissue removal is shown to be more reliable than approximation through the use of crater dimensions.

## ACKNOWLEDGMENTS

The authors thank William Gabella and John Kozub of the W. M. Keck Free-Electron Laser Center at Vanderbilt University and Marie Wilson of the Beckman Laser Institute and Medical Clinic at the University of California, Irvine, for their technical assistance. The U.S. Government is authorized to reproduce and distribute reprints for Governmental purposes notwithstanding any copyright notation. The views and conclusions contained herein are those of the authors and should not be interpreted as necessarily representing the official policies or endorsements, either expressed or implied, of the Air Force Research Laboratory or the U.S. Government.

## REFERENCES

1. Miller DV, O'Brien SJ, Arnoczky SS, Kelly A, Fealy SV, Warren RF. The use of the contact Nd:YAG laser in arthroscopic surgery: Effects on articular cartilage and meniscal tissue. Arthroscopy 1989;5:245–253.
2. Smith CF, Johansen WE, Vangsness CT, Sutter LV, Marshall GJ. The carbon dioxide laser—A potential tool for orthopedic surgery. Clin Orthop Relat Res 1989;242:43–50.
3. Trauner K, Nishioka N, Patel D. Pulsed holmium:yttrium-aluminum-garnet (Ho:YAG) laser ablation of fibrocartilage and articular cartilage. Am J Sport Med 1990;18:316–320.
4. Gonzales C, van de Merwer WP, Smith M, Reinisch L. Comparison of the Erbium-Yttrium Aluminum Garnet and carbon dioxide lasers for in vitro bone and cartilage ablation. Laryngoscope 1990;100:14–17.
5. Leunig M, Leunig A, Bise K, Goetz AE. Laser induced removal of meniscus cartilage and tendines. Lasers Med Sci 1992;7:369–374.
6. Sherk HH. Current concepts review—The use of lasers in orthopaedic procedures. J Bone Joint Surg 1993;75:768–776.
7. Shi WQ, Vari SG, Vanderveen MJ, Fishbein MC, Grundfest WS. Effect of varying laser parameters on pulsed Ho:YAG ablation of bovine knee-joint tissues. Arthroscopy 1993;9:96–102.
8. Fischer R, Hibst R, Schroder D, Puhl W, Steiner R. Thermal side effects of fiber-guided XeCl eximer laser drilling of cartilage. Lasers Surg Med 1994;14:278–286.
9. Prodoehl JA, Rhodes ALB, Cummings RS, Meller MM, Sherk HH. 308 nm eximer laser ablation of cartilage. Lasers Surg Med 1994;15:263–268.
10. Sherk HH, Black JD, Prodoehl JA, Diven J. The effect of lasers and electrosurgical devices on human meniscal tissue. Clin Orthop Relat Res 1995;310:14–20.
11. Vangsness CT, Akl T, Nelson SJ, Liaw L-HL, Smith CF, Marshall GJ. In vitro analysis of laser meniscectomy. Clin Orthop Relat Res 1995;310:21–26.
12. Vangsness CT, Watson T, Saadatmanesh V, Moran K. Pulsed Ho:YAG laser meniscectomy: Effect of pulsewidth on tissue penetration rate and lateral thermal damage. Lasers Surg Med 1995;16:61–65.

13. Trauner KB, Nishioka NS, Flotte T, Patel D. Acute and chronic response of articular cartilage to Holmium:YAG laser irradiation. Clin Orthop Relat Res 1995;310:52–57.
14. Glossop ND, Jackson RW, Koort HJ, Reed SC, Randle JA. The eximer laser in orthopedics. Clin Orthop Relat Res 1995;310:72–81.
15. Vangsness CT, Smith CF, Marshall GJ, Sweeney JR, Johansen E. The biological effects of carbon-dioxide laser surgery on rabbit articular cartilage. Clin Orthop Relat R 1995;310:48–51.
16. Bernard M, Grothues-Spork M, Hertel P, Moazami-Gourdarzi Y. Reactions of meniscal tissue after arthroscopic laser application: An in vivo study using five different laser systems. J Arth Relat Surg 1996;12:441–451.
17. Vangsness CT, Ghaderi B, Brustein M, Saadat V, Carter J. Ablation rates of human meniscal tissue with the Ho:YAG laser: The effects of varying fluences. Arthroscopy 1997;13:148–150.
18. Gonzales C, Merwe W, Smith M, Reinisch L. Comparison of the erbium-yttrium aluminum garnet and carbon dioxide lasers for in vitro bone and cartilage ablation. Laryngoscope 1990;100:14–17.
19. Frenz M, Zuger BJ, Monin D, Weiler C, Mainil-Varlet P, Weber HP, Schaffner T. Laser-induced cartilage damage: An ex-vivo model using confocal microscopy. SPIE 1999;3601:115–120.
20. Mainil-Varlet P, Monin D, Weiler C, Grogan S, Schaffner T, Züger B, Frenz M. Quantification of laser-induced cartilage injury by confocal microscopy in an ex vivo model. J Bone & Joint Surg 2001;83:566–571.
21. Vogel A, Venugopalan V. Mechanisms of pulsed laser ablation of biological tissues. Chem Rev 2003;103:577–644.
22. Edwards G, Logan R, Copeland M, et al. Tissue ablation by a free-electron laser tuned to the amide II band. Nature 1994;371:416–419.
23. Bende T, Jean B, Matallana M, Seiler T, Brau CA. Photoablation with the free-electron laser between 2.8 μm and 6.2 μm wavelength. Invest Ophth Vis Sci 1993;34:1246–1246.
24. Jean B, Bende T. Photoablation of gelatin with the free-electron laser between 2.7 μm and 6.7 μm. J Refract Corneal Surg 1994;10:433–438.
25. Bende T, Walker R, Jean B. Thermal collateral damage in porcine corneas after photoablation with free-electron laser. J Refract Surg 1995;11:129–136.
26. Peavy GM, Reinisch L, Payne JT, Venugopalan V. Comparison of cortical bone ablations by using infrared laser wavelengths 2.9 to 9.2 μm. Lasers Surg Med 1999;25:421–434.
27. Fowler WC, Rose JG, Chang DH, Proia A. The free electron laser: A system capable of determining the gold standard in laser vision correction. Nucl Instrum Meth Phy Res A 1999;429:497–501.
28. Jean B, Bende T. Mid-IR laser applications in medicine. Top Appl Phys 2003;89:511–546.
29. Edwards GS, Austin RH, Carroll FE, Copeland ML, Couprie ME, Gabella WE, Haglund RF, Hooper BA, Hutson MS, Jansen ED, et al. Free electron laser based biophysical and biomedical instrumentation. Rev Sci Instrum 2003;74:3207–3245.
30. Heya M, Fukami Y, Nagats H, Nishida Y, Awazu K. Gelatin ablation wavelength dependency in the range of 5.6–6.7 μm using a mid-infrared free electron laser. Nucl Instrum Meth Phy Res A 2003;507:564–568.
31. Mackanos MA, Kozub JA, Hachey DL, Joos KM, Ellis DL, Jansen ED. The effect of free-electron laser pulse structure on mid-infrared soft-tissue ablation: Biological effects. Phys Med Bio 2005;50:1885–1899.
32. Youn JI, Peavy GM, Venugopalan V. Free electron laser ablation of articular and fibro-cartilage at 2.79, 2.9, 6.1, and 6.45 μm: Mass removal studies. Lasers Surg Med 2005;36:202–209.
33. Gray H. Gray's anatomy. New York: Gramercy Books; 1977.
34. Caplan AI. Cartilage. Sci Am J 1984;251:84–94.
35. Naumann A, Dennis JE, Awadallah A, Carrino DA, Mansour JM, Kastenbauer E, Caplan AI. Immunochemical and mechanical characterization of cartilage subtypes in rabbit. J Histochem Cytochem 2002;50:1049–1058.
36. Simmon SR. Orthopaedic basic science. Illinois: American Academy of Orthopaedic Surgeons; 1994.
37. Hale GM, Querry MR. Optical constants of water in the 200-nm to 200-μm wavelength region. Appl Opt 1973;12:555–563.
38. Yannas IV. Collagen and gelatin in the solid state. J Macromol Sci-Revs Macromol Chem 1972;C7:49–104.
39. Cummings JP, Walsh JT. Erbium laser ablation: The effect of dynamic optical properties. Appl Phys Lett 1993;62:1988–1990.
40. Shori RK, Waltson AA, Stafsudd OM, Fried D, Walsh JT. Quantification and modeling of the dynamic changes in the absorption coefficient of water at $\lambda = 2.94$ μm. IEEE J Sel Top Quantum Electron 2001;7:959–970.
41. Duck FA. Physical properties of tissue: A comprehensive reference book. London: Academic Press; 1990. p 9–65.
42. Shapiro EM, Borthakur A, Kaufman JH, Leigh JS, Reddy R. Water distribution patterns inside bovine articular cartilage as visualized by 1H magnetic resonance imaging. Osteoarthritis Cartilage 2001;9:533–538.